Automatic Segmentation of Different Pathologies from Cardiac Cine MRI Using Registration and Multiple Component EM Estimation

Wenzhe Shi[1], Xiahai Zhuang[2], Haiyan Wang[1], Simon Duckett[3], Declan Oregan[4], Philip Edwards[1], Sebastien Ourselin[2], and Daniel Rueckert[1]

[1] Biomedical Image Analysis Group
Imperial College London
[2] Centre for Medical Image Computing
University College London
[3] The Rayne Institute
Kings College London
[4] Robert Steiner MRI Unit
Hammersmith Hospital

Abstract. In this paper, we develop a framework for the automatic detection and segmentation of the ventricle and myocardium from multi-slice, short-axis cine MR images. The segmentation framework has the ability to deal with large shape variability of the heart, poorly defined boundaries and abnormal intensity distribution of the myocardium (e.g. due to infarcts). We integrate a series of state-of-the-art techniques into a fully automatic workflow, including a detection algorithm for the LV, atlas-based segmentation, and intensity-based refinement using a Gaussian mixture model that is optimized using the Expectation Maximization (EM) algorithm and the graph cut algorithm. We evaluate this framework on three different patient groups, one with infarction, one with left ventricular hypertrophy (both are common result of cardiovascular diseases) and another group of subjects with normal heart anatomy. Results indicate that the proposed method is capable of producing segmentation results that show good robustness and high accuracy (Dice 0.908 ± 0.025 for the endocardial and 0.946 ± 0.016 for the epicardial segmentations) across all patient groups with and without pathology.

1 Introduction

Accurate estimation of indices of cardiac function, such as ejection fraction and wall thickness or thickening, is important in routine clinical applications as well as in cardiovascular research aimed at better understanding the function of the heart. In order to compute these measurements of cardiac function, one of the essential steps is to identify the ventricles and the myocardium and to delineate their boundaries. Manual segmentation tends to lead to significant inter- and intra-observer variations and is extremely time-consuming, it is hence highly desirable to develop an automated method to obtain a reproducible and unbiased result.

D.N. Metaxas and L. Axel (Eds.): FIMH 2011, LNCS 6666, pp. 163–170, 2011.

Model-based segmentation [1,2,3,4] achieves automatic delineation by deforming the surface of a pre-constructed model towards the detected boundaries, while at the same time constraining the model within a reasonable shape based on *a-priori* knowledge of the model. The detection of candidate boundaries in these methods is usually confined to a local region around the model surface. Therefore, constructing an appropriate prior model, whose shape variability can adequately capture the shape of the heart in unseen images, is crucial for segmentation techniques in this category. An alternative technique for segmentation is to propagate a pre-constructed atlas to the unseen images using image registration [5,6,7]. By using a locally affine registration method (LARM), this technique is able to deal with large shape variations of the heart. However, the segmentation accuracy reported using LARM is limited, in particular for the segmentation of the epicardium [7]. This problem becomes particularly evident when the intensities in the myocardium exhibit locally varying contrast, e.g. due to infarction.

Voxel-based segmentation identifies differences between the intensity distribution of different tissues[8,9,10,11]. The method is able to achieve sub-voxel accuracy but requires a good initialization. However, the lack of geometric information makes it difficult to achieve such a good initialization due to the large shape variation of the heart within a given population of subjects. Furthermore, most of the automatic segmentation methods, including model-based and atlas-based methods, assume homogenous tissue intensities. This leads to problems when segmenting subjects with myocardial infarction, as the infarcted myocardium often has a heterogeneous intensity distribution in contrast to normal myocardium which is characterized by a more homogeneous intensity distribution. These problems are further compounded by the fact that these heterogeneous intensity distributions are difficult model using prior knowledge since the position and intensity of infarcted myocardium varies across different subjects.

In this paper we propose an integrated framework (Figure 1) to deal with the challenges described above. This framework includes a Haar feature-based cascade classifier for heart detection, image registration for propagating prior information built from a group of healthy subjects, and a multiple component EM (MCEM) estimation and graph cut-based method for segmentation refinement. Using Gaussian mixture modelling in the EM estimation has been proposed by [12] to cope with partial volume voxels which exist at the interface between different tissue classes. We extend this approach with spatial weighting to emphasize on that the components are clustered and choose number of Gaussian models explicitly from number of potential components (for example myocardium consist of normal and infarcted myocardium and background consist of blood tissue and air).

In the following sections, the proposed method is described in Section 2, validation results are presented in Section 3, and finally the conclusion and discussion can be found in Section 4.

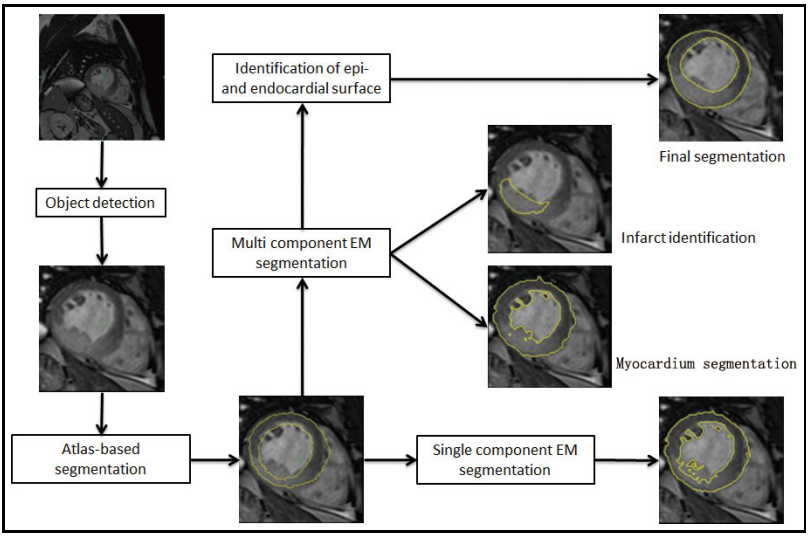

Fig. 1. Workflow of the automatic segmentation framework and MCEM against EM

2 Methods

2.1 Initial Atlas-Based Segmentation of the Heart

Once a region of interest containing the cardiac anatomy has been located via variant of the object detection approach proposed by Viola and Jones [13], we use image registration to propagate an atlas to the unseen images. Zhuang *et al.* [6,7] proposed a locally affine registration method (LARM) to address the large local shape variability of cardiac anatomy, commonly seen across large populations with pathologies. LARM is integrated into the registration process as an intermediate registration step between a global affine registration and a fully non-rigid registration. Compared to traditional registration schemes, LARM is capable of providing a good initial alignment between the images of patients with pathologies and the atlas constructed from normal subjects.

2.2 Multi-component EM Estimation

To enable voxel-based classification, we propagate a probabilistic atlas to the unseen images using the result of the previous registration process as a spatial constraint. We then use the EM algorithm [5] to classify each voxel into 3 labels $\Lambda = \{L_k, L_b, L_m\}$ for background, blood pool, and myocardium respectively. The probabilistic atlas has been constructed from 25 healthy subjects and is used as *a-priori* information for the EM algorithm. However, the probabilistic atlas has been constructed from healthy subjects. In normal anatomical MR images, the intensity of myocardium is relatively homogeneous and the EM-based segmentation is able to segment normal myocardium in healthy subjects

with high accuracy (mean distance and standard deviation reported in [5] is $2.05 \pm 2.19mm$). For the subjects with myocardial infarction, the intensity of the infarcted region can be significantly different from the healthy myocardium. This leads to inaccurate delineation of the myocardium in the infarcted region when using the traditional EM-based algorithm as the example in Figure 1 shows.

We propose to use a multiple component EM (MCEM) algorithm to cope with this abnormal intensity distribution. The MCEM algorithm models the myocardial tissue using multiple Gaussian distributions and thus can better adapt to the heterogeneous intensity distribution. Let K be the number of labels and n be the number of voxels in the image. Let $G(y_i, \mu, \sigma)$ represent a Gaussian distribution where y_i is the intensity, and μ and σ are the mean and standard deviation respectively. Furthermore let $p_L^m(i)$ be the probabilistic estimate of the segmentation of v_i for label L at the m-th iteration; $p_L^{atlas}(i)$ is the prior probability propagated from the probabilistic atlas after the registration step. The MCEM algorithm is then initialized as follows:

$$p_L^0(i) = p_L^{atlas}(i) \tag{1}$$

$$\mu_L^0 = \frac{\sum_{i=1}^n y_i p_L^0(i)}{\sum_{i=1}^n p_L^0(i)} \ , \qquad (\sigma_L^0)^2 = \frac{\sum_{i=1}^n (y_i - \mu_L^0)^2 p_L^0(i)}{\sum_{i=1}^n p_L^0(i)} \tag{2}$$

Given that label L is modelled using $|l|$ components, the initial probability segmentation of each component, $p_{L_j}^0(i)$, is given by:

$$p_{L_j}^0(i) = \frac{G(y_i, \mu_{L_j}^0, \sigma_{L_j}^0) p_L^{atlas}(i)}{\sum_{k=1}^K \sum_{o=1}^{|l|} G(y_i, \mu_{k_o}^0, \sigma_{k_o}^0) p_k^{atlas}(i)} \tag{3}$$

where $\mu_{L_j}^0 = \mu_L^0 - \sigma + \frac{2\sigma_L^0(j-1)}{|l|-1}$, $(\sigma_{L_j}^0)^2 = (\sigma_L^0)^2/|l|$, and $\delta_{L_j}^0 = \frac{\sum_i^n p_{L_j}^0(i)}{\sum_{i,o=1}^{n,|l|} p_{L_o}^0(i)}$ is the proportion of component j.

The algorithm then interleaves the following E- and M-steps:. To estimate the probabilistic segmentation, a spatial coefficient C_{Lj} which measures how close v_i is to the gravity center of label L's component j is also computed. where v_i the location of the i-th voxel This is important to avoid misclassifying similar intensities which are remote from the location of the infarction.
E-step:

$$C_{Lj} = \frac{\sum_{i=1}^n G(y_i, \mu_{L_j}^m, \sigma_{L_j}^m) p_L^{atlas}(i) v_i}{\sum_{i=1}^n G(y_i, \mu_{L_j}^m, \sigma_{L_j}^m) p_L^{atlas}(i)} \tag{4}$$

$$\omega_{L_j}^{m+1}(i) = \frac{1}{||v_i - C_{Lj}|| + 1} \tag{5}$$

$$p_{L_j}^{m+1}(i) = \frac{G(y_i, \mu_{L_j}^m, \sigma_{L_j}^m) p_L^{atlas}(i) \delta_{L_j}^m \omega_{L_j}^m(i)}{\sum_{k=1}^K \sum_{o=1}^{|l|} G(y_i, \mu_{k_o}^m, \sigma_{k_o}^m) p_k^{atlas}(i) \delta_{k_o}^m \omega_{k_o}^m(i)} \tag{6}$$

$$p_L^{m+1}(i) = \sum_{o=1}^{|l|} p_{L_o}^{m+1}(i) \tag{7}$$

M-step:

$$\mu_{L_j}^{m+1} = \frac{\sum_i^n y_i p_{L_j}^{m+1}(i)}{\sum_i^n p_{L_j}^{m+1}(i)}\ , \qquad (\sigma_{L_j}^{m+1})^2 = \frac{\sum_i^n (y_i - \mu_{L_j}^{m+1})^2 p_{L_j}^{m+1}(i)}{\sum_i^n p_{L_j}(i)^{m+1}} \tag{8}$$

$$\delta_{L_j}^{m+1} = \frac{\sum_i^n p_{L_j}^{m+1}(i)}{\sum_{i=1}^n \sum_{o=1}^{|l|} p_{Lo}^{m+1}(i)} \tag{9}$$

The EM optimization iterates until the sum of the log likelihood of the Gaussian estimation at every voxel converges and changes by less than a given small value. As a result, areas of myocardial infarction can be segmented using the Gaussian mixture model.

2.3 Segmentation of the Epi- and Endocardial Surfaces

Using the traditional EM-based segmentation, it is difficult to separate the papillary muscle from the myocardium because of the lack of tissue contrast and relatively high probability of myocardium in the area of the papillary muscle. Therefore, we propose to use an energy functions based on Markov Random Fields (MRF) in combination with graph cuts [14,10,15] to improve the smoothness of the segmentation. The data term $D_p(f_p)$ is estimated using the previous MCEM results.

To identify the endocardial contours and to remove the papillary muscle completely we computed the convex hull of the blood pool segmentation. This is done in 2D since the cardiac longitudinal contour is not always convex. Then,

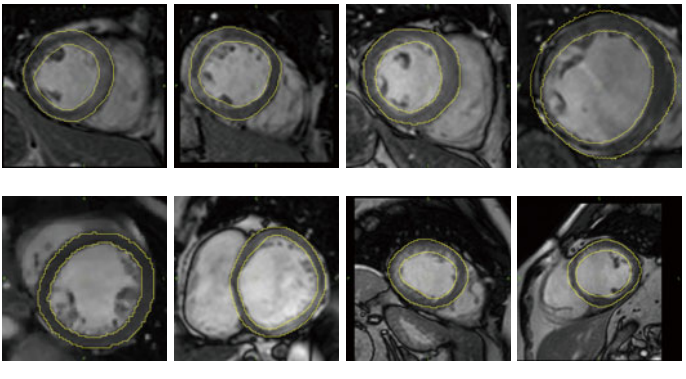

Fig. 2. Random selected segmentation results of different patients

a Fourier representation of the epi- and endocardial contour is computed and the first 6 harmonic phases are retained to obtain a final, smoothed segmentation [16,17,11]. A 3D surface model of the myocardium can be constructed using shape based interpolation [18] and marching cubes [19]. Some example of the segmentation results are shown in Figure 2.

3 Results

We acquired 90 subjects, using multi slice cine steady state free precession MR sequence acquired voxel size $1.44 \times 1.44 \times 8mm$. Images were divided into three different groups according to pathologies, including patients with myocardial infarction (49 cases), patients with ventricular hypertrophy (30 cases), and healthy subjects (11 cases). Manual segmentations were performed by a cardiologist to extract myocardium and left ventricle, and then compared to segmentation results obtained via three different techniques: (a) the technique by Lorenzo et al. [5] which uses affine and non-rigid registration of a probabilistic atlas followed by EM-MRF segmentation, (b) the technique by Zhuang et al. [6] which employs registration for atlas propagation, and (c) the technique proposed in this paper. For comparisons between the methods we used the Dice metric, $D = (2||S_a \cap S_b||)/(||S_a|| + ||S_b||)$ where S_a and S_b are the manual label segmentation and automatic label segmentation, and the surface-to-surface distance [7,20,1]. The results are summarized in Table 1 and 2.

Table 1. Validation results: The Dice overlap measure for the endocardial segmentation (L_b) and epicardial segmentation ($L_b + L_m$) results between automatic and manual segmentation"s label results

Group	Segmentation	Lorenzo et al.[5]	Zhuang et al.[7]	MCEM
normal	endocardial	0.921 ± 0.013	0.919 ± 0.016	0.927 ± 0.013
	epicardial	0.935 ± 0.016	0.936 ± 0.013	0.946 ± 0.018
infarction	endocardial	0.841 ± 0.045	0.853 ± 0.036	0.899 ± 0.029
	epicardial	0.932 ± 0.015	0.933 ± 0.012	0.950 ± 0.011
hypertrophy	endocardial	0.748 ± 0.228	0.917 ± 0.031	0.917 ± 0.028
	epicardial	0.761 ± 0.210	0.929 ± 0.028	0.940 ± 0.023

Table 2. Validation results: The average surface-to-surface distances for the endocardial surfaces and epicardial surfaces between manual and automatic segmentation"s surface results

Group	Surface	Lorenzo et al.[5]	Zhuang et al.[7]	MCEM
normal	endocardial	2.274 ± 0.115	2.119 ± 0.101	1.990 ± 0.150
	epicardial	2.154 ± 0.167	2.122 ± 0.191	1.830 ± 0.185
infarction	endocardial	2.931 ± 0.545	2.637 ± 0.590	1.926 ± 0.342
	epicardial	2.192 ± 0.325	2.326 ± 0.598	1.775 ± 0.195
hypertrophy	endocardial	6.738 ± 8.198	2.446 ± 0.459	2.349 ± 0.418
	epicardial	7.581 ± 8.073	2.862 ± 0.528	2.162 ± 0.337

The results indicate that our proposed segmentation scheme performed consistently better than the other two methods. In our experiments, the global affine registration failed for 8 out of 30 patients with ventricular hypertrophy, leading to failures using the segmentation technique proposed by Lorenzo et al. [5]. On the other side the registration-based approach by Zhuang et al. [6] uses the LARM registration technique, thus the segmentation results were significantly better on subjects with ventricular hypertrophy due to its ability to address the large local shape variability. Furthermore, the proposed method outperformed both other techniques due to its ability to model infarcted myocardium using multiple tissue class components. Finally, the MCEM segmentation achieved high accuracy for the fully automated segmentation across all three groups, which compares favourably to other recent techniques [7,20,1].

4 Discussion and Conclusion

In this paper we have developed a framework for automatic segmentation of MR images the cardiac anatomy with different pathologies. We evaluated our proposed method using a test data set with a wide diversity including healthy controls, patients with myocardial infarction and patients with cardiac myopathy. The proposed segmentation algorithm was compared to two other, state-of-the-art, segmentation schemes. The results showed a consistent improvement, particularly in the segmentation of subjects with myocardial infarction for which registration-based segmentation tends to perform poorly. Also, the voxel-based techniques[5] alone did not demonstrated a robust performance without a good initialization from LARM propagation in the group with ventricular hypertrophy. The proposed integration of registration- and voxel-based segmentation has shown the ability to achieve both the robustness and accuracy. Finally, the segmentation performance achieved by the proposed method is very competitive and outperforms some other recent approaches [7,20,1], although a direct comparison is often difficult due to the different image data sets used.

This work was funded in part by EPSRC grant EP/H019847/1.

References

1. Huang, S., Liu, J., Lee, L., Venkatesh, S., Teo, L., Au, C., Nowinski, W.: An image-based comprehensive approach for automatic segmentation of left ventricle from cardiac short axis cine mr images. Journal of Digital Imaging, 1–11 (2010) 10.1007/s10278-010-9315-4
2. Pluempitiwiriyawej, C., Moura, J., Wu, Y., Ho, C.: STACS: New active contour scheme for cardiac MR image segmentation. IEEE Transactions on Medical Imaging 24(5), 593–603 (2005)
3. Kaus, M., Berg, J., Weese, J., Niessen, W., Pekar, V.: Automated segmentation of the left ventricle in cardiac MRI. Medical Image Analysis 8(3), 245–254 (2004)
4. Rouchdy, Y., Pousin, J., Schaerer, J., Clarysse, P.: A nonlinear elastic deformable template for soft structure segmentation. Inverse Problems 23, 1017–1035 (2007)

5. Lorenzo-Valdés, M., Sanchez-Ortiz, G., Elkington, A., Mohiaddin, R., Rueckert, D.: Segmentation of 4D cardiac MR images using a probabilistic atlas and the EM algorithm. Medical Image Analysis 8(3), 255–265 (2004)
6. Zhuang, X., Rhode, K.S., Arridge, S.R., Razavi, R.S., Hill, D., Hawkes, D.J., Ourselin, S.: An atlas-based segmentation propagation framework using locally affine registration – application to automatic whole heart segmentation. In: Metaxas, D., Axel, L., Fichtinger, G., Székely, G. (eds.) MICCAI 2008, Part II. LNCS, vol. 5242, pp. 425–433. Springer, Heidelberg (2008)
7. Zhuang, X., Rhode, K., Razavi, R., Hawkes, D.J., Ourselin, S.: A Registration-Based Propagation Framework for Automatic Whole Heart Segmentation of Cardiac MRI. IEEE Transactions on Medical Imaging, 1612–1625 (2010)
8. Zhang, Y., Brady, M., Smith, S.: Segmentation of brain MR images through a hidden Markov random field model and the expectation-maximization algorithm. IEEE Transactions on Medical Imaging 20(1), 45–57 (2001)
9. Kedenburg, G., Cocosco, C.: Automatic cardiac MRI myocardium segmentation using graphcut. In: Proceedings of SPIE, vol. 6144, 61440A (2006)
10. Boykov, Y., Kolmogorov, V.: Computing Geodesics and Minimal Surfaces via Graph Cuts. In: Proceedings of the Ninth IEEE International Conference on Computer Vision, p. 26. IEEE Computer Society, Los Alamitos (2003)
11. Jolly, M.: Automatic segmentation of the left ventricle in cardiac MR and CT images. International Journal of Computer Vision 70(2), 151–163 (2006)
12. Ashburner, J., Friston, K.J.: Unified segmentation. NeuroImage 26(3), 839–851 (2005)
13. Viola, P., Jones, M.: Robust real-time object detection. International Journal of Computer Vision 57(2), 137–154 (2002)
14. Greig, D., Porteous, B., Seheult, A.: Exact maximum a posteriori estimation for binary images. Journal of the Royal Statistical Society. Series B (Methodological) 51(2), 271–279 (1989)
15. Khan, S.M., Shah, M.: A multiview approach to tracking people in crowded scenes using a planar homography constraint. In: Leonardis, A., Bischof, H., Pinz, A. (eds.) ECCV 2006. LNCS, vol. 3954, pp. 133–146. Springer, Heidelberg (2006)
16. Lu, Y., Radau, P., Connelly, K., Dick, A., Wright, G.A.: Segmentation of Left Ventricle in Cardiac Cine MRI: An Automatic Image-Driven Method. In: Ayache, N., Delingette, H., Sermesant, M. (eds.) FIMH 2009. LNCS, vol. 5528, pp. 339–347. Springer, Heidelberg (2009)
17. Huang, S., Liu, J.: Segmentation of the Left Ventricle from Cine MR Images Using a Comprehensive Approach. In: Proceedings of the 5th International Conference on Functional Imaging and Modeling of the Heart, pp. 339–347. Springer, Heidelberg (2009)
18. Grevera, G., Udupa, J.: Shape-based interpolation of multidimensional grey-level images. IEEE Transactions on Medical Imaging 15(6), 881–892 (2002)
19. Lorensen, W., Cline, H.: Marching cubes: A high resolution 3D surface construction algorithm. In: Proceedings of the 14th Annual Conference on Computer Graphics and Interactive Techniques, pp. 163–169. ACM, New York (1987)
20. Schaerer, J., Casta, C., Pousin, J., Clarysse, P.: A dynamic elastic model for segmentation and tracking of the heart in mr image sequences. Medical Image Analysis 14(6), 738–749 (2010)